 CMES, vol.19, no.1, pp.1-21, 2007

A Solenoidal Initial Condition for the Numerical Solution of the Navier-Stokes Equations for Two-Phase Incompressible Flow

F. Bierbrauer and S.-P. Zhu[1]

Abstract: Recently the use of the one-field formulation in the numerical solution of the Navier-Stokes equations for two-phase incompressible flow has become a very attractive approach in CFD (computational fluid dynamics). While the presence of material discontinuities across fluid interfaces presents some difficulty, it is their combination with a non-solenoidal discontinuous initial velocity field, commonly occurring in the mathematical formulation, that has provided the greatest hindrance in the numerical solution. This paper presents three analytical solutions, the Bounded Creeping Flow, Solenoidal and Conserved Solenoidal Solutions, which are both continuous, incompressible, retain as much of the original mathematical formulation as possible and provide a physically reasonable initial velocity field.

Keyword: solenoidal initial condition, one-field formulation, two-phase flow.

1 Introduction

The solution of free and moving boundary problems in fluid flow, encountered in the application of mathematical models in industry and the natural world, often requires the numerical solution of the incompressible Navier-Stokes (NS) equations. Such problems regularly contain multiple fluids with radically different densities and viscosities leading to material discontinuities across fluid interfaces. The solution of such problems involve either the use of multiple sets of NS equations for each fluid and solve for the fluid interfaces through application of interfacial conditions, or more recently, solve only a single NS equation which treats the density and viscosity as field variables that undergo continuous but sharp variations across the fluid interfaces. The second of these, the so-called one-field formulation, is the one that requires a special treatment of the initial condition because the combination of material discontinuities with non-solenoidal velocity discontinuities present in the problem's originally proposed initial condition has led to the greatest difficulty in the one-field formulation approach. This paper aims to resolve this issue by constructing a continuous incompressible initial velocity field valid in the entire computational domain while retaining as many of the characteristics of the original formulation as possible.

The flow of a single phase incompressible fluid within a given subdomain, usually part of the larger entire flow domain, is described by the unsteady NS equations in addition to appropriate initial and boundary conditions. Within this subdomain the physical properties of the fluid are characterized by a uniform density and viscosity. A liquid and gas may be described as continua possessing constant density and viscosity which are separated by a sharp interface with surface tension [Frohn and Roth (2000); Zhu (2001)]. This is the case in physical processes involving evaporation or condensation, that is, a phase change of a single fluid, Kothe (1999), which occurs in, for example, industrial processes such as the water-jet cooling of hot steel surfaces, Bierbrauer, Soh, and Yuen (2002), or solidification of metal in casting processes, Puckett, Almgren, Bell, Marcus, and Rider (1997). In addition, flows with multiple distinct, immiscible fluids bounded by dynamic topologically complex interfaces are also often called multiphase flows, Kothe (1999). In this case, phase refers to each distinct fluid involved, whether it is the impact of a water droplet

[1] School of Mathematics and Applied Statistics, University of Wollongong, NSW, 2522, Australia

onto a layer of liquid zinc, Bierbrauer (2004), or the wind generated waves at the air-ocean interface, Scardovelli and Zaleski (1999). The whole flow domain is separated into any number of subdomains filled with the individual phases, Scardovelli and Zaleski (1999). Each phase may then be described by a single (nonsingular) NS equation for incompressible single phase flow in addition to the appropriate conditions at the interface, Anderson, McFadden, and Wheeler (1998).[1] The material discontinuities, in density and viscosity, are here isolated within the individual phase subdomains allowing the solution of multiphase problems of zero density or viscosity within a single phase.

However, the use of multiple sets of incompressible single phase NS equations (multi-set NS) in the solution of such flow problems remains somewhat unwieldy, Frohn and Roth (2000). The variable density, incompressible, NS equations represent a natural extension of the single phase approach, described above, to the whole domain; by treating the individual material properties, density and viscosity, as field variables which undergo discontinuous jumps across material interfaces. This is the so-called one-field or one-fluid formulation, Prosperetti (2000), where each of the separate fluids move with the local center-of-mass. The multiple mass and momentum equations are replaced by a single momentum equation and a solenoidal condition on the center-of-mass velocity field, Kothe (1999). In addition to the momentum equation and the incompressibility constraint the NS equations are supplemented by two equations of state for the transport and discontinuous variation of density and viscosity over the entire domain, Vincent and Caltagirone (2000). The variable-density model allows for very large relative density ratios although any single phase density must be non-zero. The presence of surface tension at the material interfaces may be included through an extra discontinuous body force term in the momentum equations. The required interfacial conditions are a natural by-product of such a formulation, Aleinov and Puckett (1995).

The current paper considers a typical two-phase moving boundary problem using the variable density, incompressible NS equations as a suitable mathematical model. Although this approach is designed to deal with any number of fluid phases it is the two-phase case that is met with most often in the mathematical modeling of interfacial fluid flows common in industrial, technological and natural processes. One such problem is the mathematical modeling of natural or engineering processes involving the dynamic behavior of single droplets and droplet systems, Frohn and Roth (2000). There is a vast literature in this field dealing with the natural world: raindrop erosion of soil, the application of agricultural sprays for pest control, the formation of clouds; and technological applications: fuel injection in combustion engines, the delivery of aerosolized drugs for the treatment of respiratory diseases, ink-jet printing and the spray cooling of hot steel sheets, Frohn and Roth (2000).

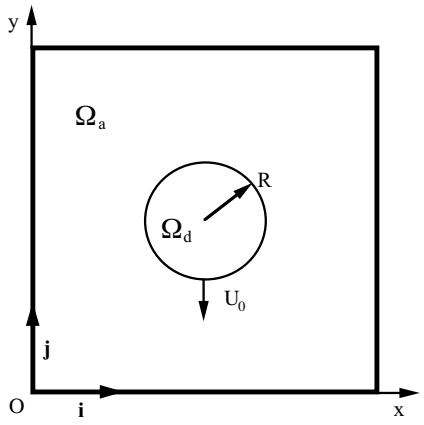

Figure 1: The spherical droplet of radius R located in Ω with initial state $\mathbf{u}_0 = -U_0\mathbf{j}$ in Ω_d and zero velocity in Ω_a

The mathematical modeling of a typical two-phase droplet problem involves the dynamic motion of a droplet of a given constant density and viscosity suspended in an ambient fluid of dra-

[1] These conditions are the stress balance: the jump in stress for nonzero surface tension or normal and shear stress continuity if the surface tension is zero; the kinematic: continuity of the normal velocity, a consequence of mass conservation; and for viscous fluids the dynamic: the continuity of tangential velocity across the interface.

matically different density and viscosity such as a water droplet in air, Puckett, Almgren, Bell, Marcus, and Rider (1997). If the domain Ω is large enough homogeneous wall conditions may be imposed at the boundary $\partial\Omega$. The initial conditions satisfied by this kind of problem really exists as two different states. The first is what will here be called the (discontinuous) *initial state* of the problem which is usually defined by a given constant, non-zero initial velocity of the droplet (d) $\mathbf{u}(\mathbf{x},0) = -U_0\mathbf{j}$ in Ω_d while surrounded by the second stationary ambient (a) fluid $\mathbf{u}(\mathbf{x},0) = \mathbf{0}$ in Ω_a, see Figure 1. This problem demonstrates both velocity and material singularities, an unacceptable situation even for the multi-set NS equations. The second state is the true *initial condition* of the problem $\mathbf{u}_0(\mathbf{x})$ in $\overline{\Omega}$ which must satisfy the incompressibility constraint globally, Gresho (1991). Here, $\Omega \equiv \Omega_d \cup \Omega_a$ and $\overline{\Omega} \equiv \Omega \cup \partial\Omega$. In summary, for $t > 0$:

$$\nabla \cdot \mathbf{u} = 0 \quad \text{in} \quad \overline{\Omega} \tag{1}$$

subject to the boundary condition for $t > 0$:

$$\mathbf{u} = \mathbf{0} \quad \text{on} \quad \partial\Omega \tag{2}$$

and the actual initial condition:

$$\mathbf{u}(\mathbf{x},0) = \mathbf{u}_0(\mathbf{x}) \quad \text{in} \quad \overline{\Omega} \tag{3}$$

where:

$$\nabla \cdot \mathbf{u}_0 = 0 \quad \text{in} \quad \Omega \tag{4}$$

and, with outward normal $\mathbf{n}$:

$$\mathbf{n} \cdot \mathbf{u}_0 = 0 \quad \text{on} \quad \partial\Omega \tag{5}$$

Note that the normal component of (2) is in fact (1) on $\partial\Omega$ so that with (4) and (5) the equations (1)-(5) simply read, Gresho (1992):

$$\nabla \cdot \mathbf{u} = 0 \quad \text{in} \quad \overline{\Omega} \quad \text{for} \quad t \geq 0 \tag{6}$$

This is equivalent to stating that the velocity field is always and everywhere incompressible, Gresho (1991). Two direct consequences of this are that there are constraints on the initial data (4) and that impulsive starts are precluded, Gresho and Sani (1987). In addition, if (4) and/or (5) are/is violated the problem becomes ill-posed, Temam (1985). It is clear that the initial state does not satisfy (4), see Appendix A:, so that the problem is both ill-posed and does not satisfy the incompressibility constraint.[2]

The consequences of the incompressibility constraint also carry over into the numerical solution of the two-phase, variable density, NS equations, Gresho (1992). The construction of practical numerical methods for the solution of multiphase interfacial flow problems has veered away from moving grid Lagrangian methods to fixed grid Eulerian methods, Kothe (1999). In contrast to Lagrangian methods, whose solution accuracy and robustness tend to deteriorate in proportion to the complexity of the interface topology, Kothe (1999), the Eulerian approach allows the direct numerical simulation of multi-phase flows to be easily coded when the interface is strongly distorted, Vincent and Caltagirone (2000). A properly constructed Eulerian method has the ability to be accurate, robust, and of high fidelity, Kothe and Rider (1995).[3] The main difficulty in solving the time dependent NS equations in primitive variable form is that the velocity and pressure are intimately coupled, Gresho (1990). Chorin (1968), noted that for incompressible flows the pressure is not a true thermodynamic variable and acts only as a Lagrange multiplier which ensures solenoidality. An attempt at decoupling the pressure and velocity variables is possible through a two-step predictor-corrector procedure by selecting a non-solenoidal intermediate velocity field, obtained from the momentum equations, followed by a projection onto the nearest divergence free subspace. This is made possible through the Helmholtz decomposition, Sohr (2000), of a vec-

[2] An associated well-posed problem may be constructed by projecting the nonsolenoidal velocity field onto a nearby div-free subspace, see equations (7)-(10).

[3] *accurate*: in terms of a reasonable level of measured error in the solution, *robust*: or an ability to generate physically reasonable solutions beyond the point at which accuracy is expected to be achieved, *high fidelity*: a method which produces accurate solutions relative to the computational resources allocated to it, Kothe and Rider (1995).

tor field and its associated (elliptic) Neumann problem, Quartapelle (1993).

Building upon Chorin's classical exact projection method, where the discrete projection operator behaves similarly to the analytic operator, Bell, Colella, and Glaz (1989), demonstrated the ability of projection methods to accurately solve the constant density NS equations. This was extended to the variable density case by Bell and Marcus (1992), allowing the method to model interfacial flow problems with large density jumps. However, numerical instabilities associated with local grid decoupling present in (constant density) exact projection methods motivated the development of so-called approximate projection methods, Almgren, Bell, and Szymczak (1996), which allowed for small non-solenoidal velocity fields of the same order of the spatial truncation error of the numerical method, Kothe (1999). The extension to the variable density approximate projection case by Rider and coworkers [Puckett, Almgren, Bell, Marcus, and Rider (1997); Rider (1994); Rider, Kothe, Mosso, Cerutti, and Hochstein (1995)] provided a very robust and accurate numerical method to solve the Navier-Stokes equations for multiphase flows.

The projection itself is carried out by subtracting off the non-solenoidal part of the given velocity field $\mathbf{u}(\mathbf{x})$ through the Helmholtz decomposition. Any vector may be decomposed into the sum of a divergence free, $\mathbf{u}^d(\mathbf{x})$, and curl free, $\nabla\varphi$, component. This involves the solution of a Poisson equation for $\varphi(\mathbf{x})$:

$$\nabla\cdot\sigma\nabla\varphi = \nabla\cdot\mathbf{u}_0 \quad \text{in } \Omega \tag{7}$$

subject to Neumann boundary conditions:

$$\mathbf{n}\cdot\nabla\varphi = 0 \quad \text{on } \partial\Omega \tag{8}$$

Given a discontinuous, non-solenoidal velocity field $\mathbf{u}_0$ present in the initial state, Appendix A:, a divergence free initial velocity field $\mathbf{u}_0^d$ could be obtained through the projection (7), (8), where the boundary conditions of (1)-(5) have been used, followed by the correction, Bell and Marcus (1992):

$$\mathbf{u}_0^d = \mathbf{u}_0 - \sigma\nabla\varphi \quad \text{in } \overline{\Omega} \tag{9}$$

This also initializes the pressure field

$$p(\mathbf{x}) = \varphi(\mathbf{x}) \tag{10}$$

where $\sigma(\mathbf{x}) = 1/\rho(\mathbf{x})$ is the inverse of the density field.

Although approximate projection methods are robust, and often lead to very accurate solutions of interfacial flow problems, the initial second order error $\nabla\cdot\mathbf{u}_0^d \simeq O(h^2)$ obtained from a discrete version of the projection (7)-(9) should both maintain the same order of error and, more importantly, not grow, Rider (1994).[4] If these divergent modes are ignored, especially in the presence of large density jumps, solution quality can markedly deteriorate, Kothe (1999), and lead to instability. In order that the numerical solution of the two-phase, incompressible, variable density NS equations maintains an (almost) solenoidal velocity field for each time-step we wish to ensure that any errors carried forward in the calculation do not arise from the initial condition.

Recent research has shown that the attempt to ensure a solenoidal velocity field through the numerical solution of the system (7), (8) with discontinuous (inverse) density coefficients often requires highly specialized discretisations of the elliptic operator $\nabla\cdot\sigma\nabla$, [Hyman, Shashkov, and Steinberg (1997); Li (1994); Wang (2004)]. In addition, numerical calculations show that the solution of the Neumann problem (7), (8) gets progressively more difficult as the (discontinuous) divergence term on the right hand side deviates from zero, Bierbrauer (2004).

It is the aim of this paper to construct a divergence free initial velocity field without recourse to the projection (7)-(9) but rather by an analytically derived initial velocity field which possesses the four characteristics: (i) being divergence-free over the whole domain Ω, (ii) a uniform vertical velocity $\mathbf{u}_0 = -U_0\mathbf{j}$ in Ω_d, (iii) homogeneous wall boundary conditions and (iv) a physically reasonable representation of the initial condition used for any subsequent flow calculations.

[4] This occurs when the null space of the discrete divergence $D\cdot\mathbf{u}_0$ is not allowed to grow. These are the spatial modes that are not solenoidal, $\nabla\cdot\mathbf{u}\neq 0$, although the discrete operator does not 'see' them i.e. it obtains $D\cdot\mathbf{u} = 0$.

2 Dynamic, Kinematic and Semi-Dynamic Solutions

Three avenues are open for such an analytic incompressible initial velocity field. The first considers a *dynamic* solution of the NS equations involving as much of the real dynamics of the problem as possible, i.e. all of the four characteristics (i)-(iv). The second, a purely *kinematic* solution, requires a velocity field which satisfies only the div-free constraint, a uniform vertical droplet velocity and zero wall boundary conditions i.e. characteristics (i)-(iii). Finally, the third, a *semi-dynamic* solution which, in addition to the characteristics of the kinematic solution involve aspects of the dynamics such as mass and momentum conservation without direct use of the momentum equations.

Although the first of these provides the most physically realistic initial condition it is also the most difficult to solve of all of them. Unless the geometry of the problem is simple enough its solution must rely on a numerical solution which possesses its own serious difficulties including discontinuous velocity, viscosity and density fields. The kinematic solution on the other hand only considers a solution to the divergence free constraint equation (6) and is consequently far easier to solve, even in more complicated geometries. The semi-dynamic solution combines aspects of both of the first two without making use of the momentum equations themselves although requiring extra integral constraint equations. Although it appears more analytically tractable than the dynamic solution it also possesses certain disadvantages as will be seen in Section 2.4. These solution types are here called droplet initialization problems.

2.1 The Droplet Initialization Problem

The problem, with $x-y$ coordinate system as shown in Figure 1, is first simplified so that the original domain Ω is restricted to a two dimensional spherical droplet of inner radius r_i, constant density ρ_i, constant viscosity μ_i and uniform inner velocity $\mathbf{u}^{(i)}(x,y) = -U_0\mathbf{j}$ such that the velocity boundary condition is given by $\mathbf{u}^{(i)}(r_i,\theta) = -U_0\mathbf{j}$. This, *inner droplet*, is surrounded by a stationary ring of outer fluid of constant density $\rho_o < \rho_i$, constant viscosity $\mu_o < \mu_i$, for $r_i \le r \le r_o$ and outer boundary condition $\mathbf{u}^{(o)}(r_o,\theta) = \mathbf{0}$. The extension of the inner droplet including the outer ring will also be called the *outer droplet*. The choice of outer ring rather than an unbounded domain is essential as any asymptotic solution generally does not decay to zero within only a few droplet radii which, in many situations, as well as the present one, remains the case. A non-zero velocity at the domain boundary $\partial\Omega$, which is a direct consequence of an asymptotic solution in a bounded domain, merely shifts the velocity discontinuity present in the initial state (at the droplet-ambient interface) and does not completely remove it. Although there exists a sharp density and viscosity jump between the two media at $r = r_i$ the outer ring serves as a matching domain for the inner and outer velocity boundary conditions. Note that this outer ring of width $r_o - r_i$ should be reasonably narrow so as to retain as much of the initial state characteristics as possible. The initial state described above will be called the *original droplet* (OD) problem and is shown in Figure 2(a).

On the other hand it is also possible to overcome the sharp density discontinuity by postulating a *modified droplet* problem with a gradually varying density and a continuous velocity field extending from the center of the droplet to the outer radius r_o while retaining the zero outer boundary condition $\mathbf{u}(r_o,\theta) = \mathbf{0}$. This takes place over an extra ring of fluid interspersed between the original inner and outer fluids such that the original droplet of density ρ_i is now reduced in radius i.e. $0 \le r \le \alpha$ while the middle ring ranges from $\alpha < r \le \beta$ and possesses a varying density $\rho(r)$. This middle ring is of width $\beta - \alpha$ and provides a transition length, which upon discretization of the mathematical model, may be several integer multiples of the (computational) cell width h. The outer ring of fluid of density ρ_o now covers the range $\beta < r \le r_o$. The geometry of the modified droplet problem is shown in Figure 2(b).

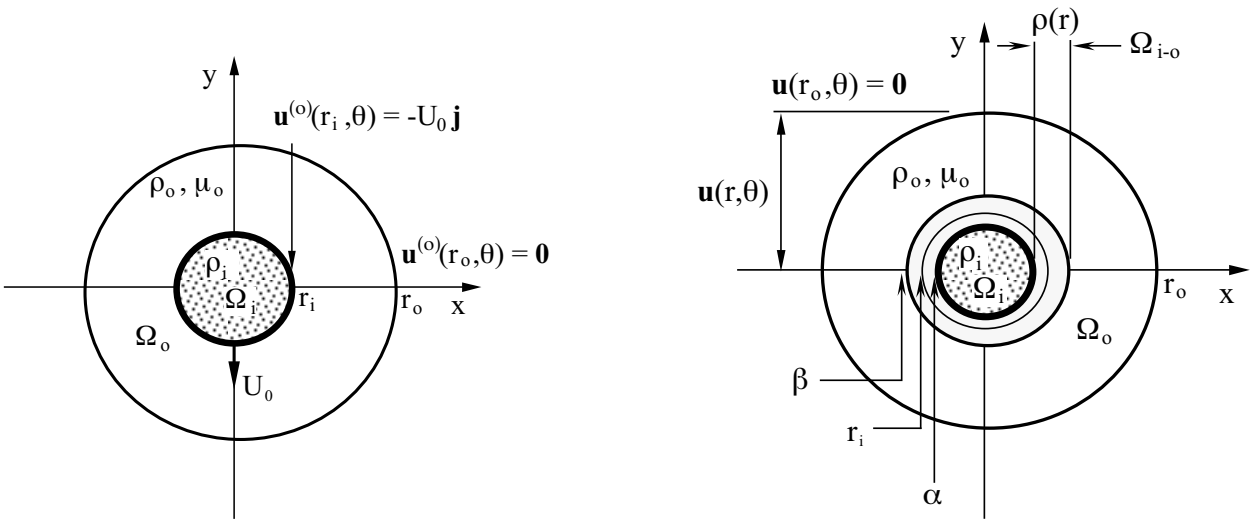

(a) the original droplet (b) the modified droplet

Figure 2: The two droplet problems in a droplet-centered frame: (a) the original droplet of radius r_i, density ρ_i and velocity $\mathbf{u}^{(i)}(r,\theta) = -U_0\mathbf{j}$ surrounded by an outer fluid ring, $r_i < r \le r_o$, of density ρ_o and zero velocity, $\mathbf{u}^{(o)}(r,\theta) = \mathbf{0}$ (b) a modification of the original droplet now of varying velocity $\mathbf{u}(r,\theta)$ for all $0 \le r \le r_o$, density ρ_i in $0 \le r \le \alpha$ followed by a ring, $\alpha \le r \le \beta$, with varying density $\rho = \rho(r)$ and an outer ring, $\beta \le r \le r_o$, of density ρ_o with boundary condition $\mathbf{u}(r_o,\theta) = \mathbf{0}$.

The spherical character of the droplet configuration suggests the use of polar coordinates as the most natural way to analyze the initialization problem. Consider the droplet centered in an $x-y$ frame with radial coordinate r and angular coordinate θ with all fluid dynamical variables expressed in polar coordinates such that $\mathbf{u} = \mathbf{u}(r,\theta)$, $p = p(r,\theta)$. The uniformity of the droplet velocity suggests the simplification, Leal (1992):

$$\begin{aligned} u_r(r,\theta) &= U(r)\sin\theta, \\ u_\theta(r,\theta) &= \Theta(r)\cos\theta, \\ p(r,\theta) &= P_0 + P(r)\sin\theta \end{aligned} \tag{11}$$

for P_0 an arbitrary constant pressure.

2.2 The Bounded Creeping Flow Solution

An example of a relatively simple and analytically tractable dynamic solution is the well-known Creeping Flow Solution for the steady motion of a solid translating sphere through an unbounded quiescent fluid, Happel and Brenner (1991). This is particularly useful for the present case as the solid sphere approximates a droplet of uniform initial velocity. Although the creeping flow limit assumes that the inertial motion of the sphere is insignificant compared to the viscous forces acting it still provides a convenient analytical solution for the current problem.

The use of the creeping flow reduction is here modified to deal with a translating fluid sphere of uniform vertical velocity surrounded by a bounded domain. The asymptotic nature of the original creeping flow solution no longer applies and is replaced by two sets of creeping flow equations for the inside of the droplet and the outer ring of ambient fluid with appropriate velocity boundary conditions at the inner and the outer radius, see Figure 2(a). It is important to retain as much of the original droplet problem characteristics as possible including the concentration of mass and momentum as close as possible to the central droplet with its uniform vertical velocity. This is also the reason why a translated solid, rather than, fluid sphere has been chosen as the representation of the creeping flow solution. Note that this approach is somewhat unphysical given that the solid sphere is now a droplet and that the asymptotic aspects are replaced by a finite radial

boundary condition. Nevertheless, the aim is to obtain a divergence-free velocity field as an initial condition for which this method is both simple and ideally suited.

This method, the first of the initialization problems, will henceforth be called the *Bounded Creeping Flow Solution* (BCFS). The problem to be solved involves the flow both inside (i) and outside (o) the droplet so that there exist two problems defined by

$$\mu^{(i)}\nabla^2\mathbf{u}^{(i)} = \nabla p^{(i)}, \quad \nabla\cdot\mathbf{u}^{(i)} = 0 \quad \text{in } \Omega_i \tag{12}$$

$$\mu^{(o)}\nabla^2\mathbf{u}^{(o)} = \nabla p^{(o)}, \quad \nabla\cdot\mathbf{u}^{(o)} = 0 \quad \text{in } \Omega_o \tag{13}$$

2.2.1 Inside the Droplet

The simplest approach makes use of polar coordinates defined in Appendix B:. Inside the droplet the solution to the NS equations (12) is a constant velocity, such that in polar coordinates:

$$u_r^{(i)}(r,\theta) = -U_0\sin\theta, \quad u_\theta^{(i)}(r,\theta) = -U_0\cos\theta, \tag{14}$$

$$p^{(i)}(r,\theta) = 0 \tag{15}$$

where $U(r) = -U_0$, $\Theta(r) = -U_0$ and $P_0 = P(r) = 0$ for $0 \le r < r_i$. Or equivalently in $x-y$ coordinates:

$$u_x^{(i)}(x,y) = 0, \quad u_y^{(i)}(x,y) = -U_0, \quad p^{(i)}(x,y) = 0 \tag{16}$$

with its associated stream function:

$$\Psi^{(i)}(x,y) = U_0 x = U_0 r\cos\theta \tag{17}$$

2.2.2 Outside the Droplet

Solve the NS equations (13) in polar coordinates, for $r_i \le r \le r_o$:

$$\mu^{(o)}\left[\frac{1}{r}\frac{\partial}{\partial r}\left(r\frac{\partial u_r^{(o)}}{\partial r}\right) + \frac{1}{r^2}\frac{\partial^2 u_r^{(o)}}{\partial\theta^2} - \frac{2}{r^2}\frac{\partial u_\theta^{(o)}}{\partial\theta} - \frac{u_r^{(o)}}{r^2}\right] = \frac{\partial p^{(o)}}{\partial r}$$

$$\mu^{(o)}\left[\frac{1}{r}\frac{\partial}{\partial r}\left(r\frac{\partial u_\theta^{(o)}}{\partial r}\right) + \frac{1}{r^2}\frac{\partial^2 u_\theta^{(o)}}{\partial\theta^2} + \frac{2}{r^2}\frac{\partial u_r^{(o)}}{\partial\theta} - \frac{u_\theta^{(o)}}{r^2}\right] = \frac{1}{r}\frac{\partial p^{(o)}}{\partial\theta}$$

$$\frac{\partial}{\partial r}(ru_r^{(o)}) + \frac{\partial u_\theta^{(o)}}{\partial\theta} = 0$$

subject to the boundary conditions at $r = r_i$ and $r = r_o$:

$$u_r^{(o)}(r_i,\theta) = -U_0\sin\theta, \quad u_\theta^{(o)}(r_i,\theta) = -U_0\cos\theta$$
$$u_r^{(o)}(r_o,\theta) = 0, \qquad u_\theta^{(o)}(r_o,\theta) = 0$$

substituting (11) we obtain a set of three ODE's for $U^{(o)}$, $\Theta^{(o)}$ and $P^{(o)}$:

$$\mu^{(o)}\sin\theta\left[\frac{d^2U^{(o)}}{dr^2} + \frac{1}{r}\frac{dU^{(o)}}{dr} - \frac{2U^{(o)}}{r^2} + \frac{2\Theta^{(o)}}{r^2}\right] = \sin\theta\frac{dP^{(o)}}{dr} \tag{18}$$

$$\mu^{(o)}\cos\theta\left[\frac{d^2\Theta^{(o)}}{dr^2} + \frac{1}{r}\frac{d\Theta^{(o)}}{dr} - \frac{2\Theta^{(o)}}{r^2} + \frac{2U^{(o)}}{r^2}\right] = \cos\theta\frac{P^{(o)}}{r} \tag{19}$$

$$\frac{dU^{(o)}}{dr} = \frac{\Theta^{(o)} - U^{(o)}}{r} \tag{20}$$

canceling $\sin\theta$ in (18) and $\cos\theta$ in (19), differentiating (19) with respect to r to eliminate $P^{(o)}(r)$ and using (20) we get:

$$U^{(o)}(r) = c_1 + c_2\ln r + c_3 r^2 + \frac{c_4}{r^2} \tag{21}$$

$$\Theta^{(o)}(r) = c_1 + c_2 + c_2\ln r + 3c_3 r^2 - \frac{c_4}{r^2} \tag{22}$$

$$P^{(o)}(r) = -\frac{2\mu^{(o)}}{r}(c_2 - 4c_3 r^2) \tag{23}$$

subject to:

$$U^{(o)}(r_i) = -U_0, \quad \Theta^{(o)}(r_i) = -U_0$$
$$U^{(o)}(r_o) = 0, \qquad \Theta^{(o)}(r_o) = 0$$

a set of four equations in four unknown constants: c_1, c_2, c_3, c_4. The solutions for $U^{(o)}$, $\Theta^{(o)}$ and $P^{(o)}$ are, ($a = \ln r_o - \ln r$, $b = \ln r_o - \ln r_i$):

$$U^{(o)}(r) = \frac{-\{r^4 + [(2a-1)r_o^2 + (2a+1)r_i^2]r^2 - r_i^2 r_o^2\}U_0}{2r^2[(b-1)r_o^2 + (b+1)r_i^2]}$$

$$\Theta^{(o)}(r) = \frac{-\{3r^4 + [(2a-3)r_o^2 + (2a-1)r_i^2]r^2 + r_i^2 r_o^2\}U_0}{2r^2[(b-1)r_o^2 + (b+1)r_i^2]}$$

$$P^{(o)}(r) = \frac{-2\mu^{(o)}(r_o^2 + r_i^2 + 2r^2)U_0}{r[(b-1)r_o^2 + (b+1)r_i^2]}$$

so that:

$$u_r^{(o)}(r,\theta) = U^{(o)}(r)\sin\theta,$$
$$u_\theta^{(o)}(r,\theta) = \Theta^{(o)}(r)\cos\theta,$$
$$p^{(o)}(r,\theta) = P_0 + P^{(o)}(r)\sin\theta$$

and that at the surface of the droplet $u_r^{(o)}(r_i,\theta) = -U_0$, $u_\theta^{(o)}(r_i,\theta) = -U_0$ with a non-zero pressure given by

$$p^{(o)}(r_i,\theta) = P_0 - \frac{2\mu^{(o)}(r_o^2 + 3r_i^2)U_0\sin\theta}{r_i[(b-1)r_o^2 + (b+1)r_i^2]}$$

which decreases, at $r = r_o$, to:

$$p^{(o)}(r_o,\theta) = P_0 - \frac{2\mu^{(o)}(3r_o^2 + r_i^2)U_0\sin\theta}{r_o[(b-1)r_o^2 + (b+1)r_i^2]}$$

The solutions in $x-y$ coordinates read:

$$u_x^{(o)}(x,y) = \frac{xy[r^4 - (r_i^2 + r_o^2)r^2 + r_i^2 r_o^2]U_0}{[(b-1)r_o^2 + (b+1)r_i^2]r^4}$$

$$u_y^{(o)}(x,y) = \Big\{r^6 + \left[2x^2 + 2r_s^2 a + r_i^2 - r_o^2\right]r^4 - \left[r_i^2 r_o^2 + 2x^2 r_s^2\right]r^2 + 2x^2 r_i^2 r_o^2\Big\}U_0 \Big/ 2\left[(b-1)r_o^2 + (b+1)r_i^2\right]r^4$$

$$p^{(o)}(x,y) = P_0 - \frac{2\mu^{(o)}y(r_o^2 + r_i^2 + 2r^2)U_0}{r^2[(b-1)r_o^2 + (b+1)r_i^2]}$$

with $r = \sqrt{x^2+y^2}$ and $r_s^2 = r_i^2 + r_o^2$. The associated stream function is calculated from:

$$\Psi^{(o)}(r,\theta) = -\int_{r_i}^{r} u_\theta^{(o)}(\xi,\theta)\,d\xi + U_0 r_i\cos\theta$$

using the fact that $\Psi^{(o)}(r_i,\theta) = \Psi^{(i)}(r_i,\theta) = U_0 r_i\cos\theta$, from (17). That is:

$$\Psi^{(o)}(x,y) = \frac{x\{r^4 + [2(r_i^2 + r_o^2)a + r_i^2 - r_o^2]r^2 - r_i^2 r_o^2\}U_0}{2[(b-1)r_o^2 + (b+1)r_i^2]r^2} \quad (24)$$

2.2.3 Restriction on r_o

Given that the velocity at $r = r_o$ is artificially truncated to zero it is advisable to ensure that at no point does the velocity field outside the droplet exceed that of the droplet itself. That is, it is required that:

$$\max_{\substack{r_i \le r \le r_o \\ 0 \le \theta \le 2\pi}} |\mathbf{u}^{(o)}(r,\theta)| \le U_0$$

where $|\mathbf{u}^{(o)}| = \sqrt{U^{(o)2}\sin^2\theta + \Theta^{(o)2}\cos^2\theta}$. In the case of $U^{(o)}(r)$ it is straightforward to show that for $r_o > r_i$ the only turning points are a minimum at $r = r_i$ and a maximum at $r = r_o$. So the slope $dU^{(o)}(r)/dr > 0$ in $r_i < r < r_o$. The function $U^{(o)}(r)$ is always increasing in this range. However, $\Theta^{(o)}(r)$ possesses a single turning point in this range given by $r = \sqrt{6(r_o^2 + r_i^2) + 6\sqrt{(r_o^2 + r_i^2) + 12r_o^2 r_i^2}/6}$ as well as a local minimum at $r = r_i$ and $\Theta^{(o)}(r_o) = 0$. This is a maximum in the range $r_i < r < r_o$. To ensure that the maximum magnitude of the velocity does not exceed U_0 in this range it is found that $r_o \ge 2.868 r_i$ approximately.

2.3 The Solenoidal Solution

This, the second of the initialization problems, is a purely kinematic solution to the div-free problem, or a purely *Solenoidal Solution* (SS), with identical boundary conditions to the BCFS and the same solution inside the droplet. It is purely kinematic and so only involves the solution of the div-free constraint without use of the momentum equations.

Reducing the original div-free constraint in polar coordinates (50) with the simplification (11) the ordinary differential equation reads:

$$\frac{d}{dr}\left(rU^{(o)}(r)\right) = \Theta^{(o)}(r)$$

subject to

$$U^{(o)}(r_i) = -U_0, \quad \Theta^{(o)}(r_i) = -U_0$$
$$U^{(o)}(r_o) = 0, \qquad \Theta^{(o)}(r_o) = 0$$

from the above ODE and the given boundary conditions the problem reduces to the solution of the integral:

$$U^{(o)}(r) = \frac{1}{r}\int_{r_i}^{r} \Theta^{(o)}(\xi)\, d\xi - \frac{U_0 r_i}{r} \tag{25}$$

for a given $\Theta^{(o)}(r)$, $U^{(o)}(r_o) = 0$, $\Theta^{(o)}(r_i) = -U_o$ and $\Theta^{(o)}(r_o) = 0$. Proposing a polynomial solution of the type $\Theta^{(o)}(r) = -(r_o - r)(a_0 + a_1 r)$ for some constants a_i, applying the boundary conditions the solutions are:

$$U^{(o)}(r) = \frac{-(r_o - r)^2[(r_i + r_o)r - 2r_i^2]U_0}{(r_o - r_i)^3 r},$$

$$\Theta^{(o)}(r) = \frac{-(r_o - r)[(r_o - r_i)^2 - 3(r_i + r_o)(r - r_i)]U_0}{(r_o - r_i)^3}$$

The equivalent components in $x - y$ coordinates are, using (49):

$$u_x^{(o)}(x,y) = \frac{-2xy(r_o - r)(r - r_i)[(r_i + r_o)r + r_i r_o]U_0}{(r_o - r_i)^3 r^3} \tag{26}$$

$$u_y^{(o)}(x,y) = (r_o - r)\Big[ar^4 - br^3 + 2(r_i^2 r_o + ax^2)r^2 - 2r_i^2 x^2 r - 2r_o r_i^2 x^2\Big]U_0 \Big/ (r_o - r_i)^3 r^3 \tag{27}$$

where the constants a, b are given by:

$$a = r_i + r_o, \quad b = r_o^2 + r_i r_o + 2r_i^2$$

with the associated stream function:

$$\Psi^{(o)}(x,y) = \frac{x(r_o - r)^2[(r_i + r_o)r - 2r_i^2]U_0}{(r_o - r_i)^3 r} \tag{28}$$

Note that a pressure field may be found through the use of the steady NS equations. The option of solving (7), (8) exists although the solution will be a constant pressure since the solenoidal solution (26), (27) is exactly div-free.

2.3.1 Restriction on r_o

Again, $dU^{(o)}(r)/dr > 0$ in the range $r_i < r < r_o$ so that it is always an increasing function of r. On the other hand $d\Theta^{(o)}(r)/dr$ is positive in the range $r_i < r < r_{tp}$ and negative over $r_{tp} < r < r_o$, where r_{tp} is a turning point located at $r_{tp} = 2(r_o^2 + r_i r_o + r_i^2)/3(r_i + r_o)$ so that $\Theta^{(o)}(r_{tp}) = (r_o + 2r_i^2)U_0/3(r_o^2 - r_i^2)$. The maximum size of $\Theta^{(o)}(r_{tp})$ stays below U_0 provided:

$$r_o > \left(1 + \frac{3}{\sqrt{2}}\right) r_i$$

2.4 The Conserved Solenoidal Solution

This third type of initialization problem solution, the semi-dynamic solution, is one of the most general taking into account continuous density variation from an *inner droplet* of constant density ρ_i and radius α out to $r = \beta$ followed by an *outer ring* of density ρ_o and outer radius r_o. The velocity field is allowed to vary from the center of the droplet out to the outer radius, this allows continuity in both density and velocity fields as well as incompressibility. This implies that this third problem type solves for the velocity in the entire domain so that the inner and outer problem are now one problem with $\mathbf{u} = \mathbf{u}(r, \theta)$ in $0 \le r \le r_o$. The degree of freedom possible in these problems is such that these attempts remain three of a whole family of solutions possible with the given conditions.

2.4.1 Conservation Equations

Although the modified droplet problem as stated in the previous paragraph is an artificial one, it is advantageous to try to maintain as many physical characteristics as possible. Certainly, total mass must be conserved over the inner droplet and outer ring. In addition, it is advantageous to conserve momentum both as a realistic physical property as well as enforcing the correct velocity direction in the outer ring, this would not be the case

if kinetic energy were used instead. Here, *conservation of momentum*, does not refer to a conservation over time, rather it refers to an equality of the total momentum in the modified droplet problem and the original droplet problem over the entire domain Ω. As such, this problem will be called the *Conserved Solenoidal Solution* (CSS).

1. The Original droplet: We have from Figure 2(a) (original droplet) in regions Ω_i and Ω_o:

   total mass

   $$\rho_i \pi r_i^2 + \rho_o \pi (r_o^2 - r_i^2)$$

   total x-momentum

   $$0$$

   total y-momentum

   $$-\rho_i \pi r_i^2 U_0$$

   Given that both velocity and density may vary throughout the domain $\Omega = \Omega_i \cup \Omega_{i-o} \cup \Omega_o$, the problem may be further simplified by noting that dimensionally speaking most of the mass and momentum of the original droplet is confined to the inner region Ω_i. For example: for a water droplet in air the mass in Ω_i is $m_i = 1000\ \pi r_i^2$ kg and in Ω_o is $m_o = 1\ \pi(r_o^2 - r_i^2)$ kg, a ratio of $1000/[(r_o/r_i)^2 - 1]$. This ratio only approaches unity for large $r_o \sim 30 r_i$. Similarly, the momentum in Ω_i is $10000 \pi r_i^2$ kg m/s whereas in Ω_o it is zero. This implies that it is best to confine most of the momentum and mass within a droplet of roughly the same size, density and velocity which still allows both density and velocity continuity throughout the whole domain. Thus a structure such as that shown in Figure 2(b) probably provides the optimum geometry for these requirements.[5]

[5] N.B. since the current method deals with the impact of immiscible fluids sharp density interfaces are maintained throughout, this implies that any density variation defined over a region is carried forward in the calculation and is maintained. A density variation which attempts to maintain an approximately sharp interface best suits the current problem. Therefore the region $\Omega_{i-o} = \{(r,\theta) : \alpha \le r \le \beta, 0 \le \theta \le 2\pi\}$ should be kept relatively thin.

2. The Modified droplet: The domain of the modified droplet consists of a central droplet, Ω_i, of density ρ_i, radius α, surrounded by a concentric ring, Ω_{i-o}, of density $\rho_{i-o} = \rho(r)$, width $\beta - \alpha$, varying velocity $\mathbf{u}_{i-o} = \mathbf{u}(r,\theta)$ also enclosed within a second ring, Ω_o, of density ρ_o, width $r_o - \beta$ and velocity approaching zero at the boundary of the domain i.e. $\mathbf{u}(r_o,\theta) = \mathbf{0}$.

   Therefore:

   total mass

   $$\rho_i \pi \alpha^2 + \int_{\Omega_{i-o}} \rho(x,y)\, dA + \rho_o \pi (r_o^2 - \beta^2)$$

   total x-momentum

   $$\rho_i \int_{\Omega_i} u_x(x,y)\, dA + \int_{\Omega_{i-o}} \rho(x,y) u_x(x,y)\, dA + \rho_o \int_{\Omega_o} u_x(x,y)\, dA$$

   total y-momentum

   $$\rho_i \int_{\Omega_i} u_y(x,y)\, dA + \int_{\Omega_{i-o}} \rho(x,y) u_y(x,y)\, dA + \rho_o \int_{\Omega_o} u_y(x,y)\, dA$$

   Using the simplifications (11), in polar coordinates we have:

   total mass

   $$\rho_i \pi \alpha^2 + \int_0^{2\pi} \int_\alpha^\beta \rho(r)\, r dr d\theta + \rho_o \pi (r_o^2 - \beta^2)$$

   total x-momentum

   $$\frac{\rho_i}{2} \int_0^{2\pi} \int_0^\alpha [U - \Theta] \sin 2\theta\, r dr d\theta + \frac{1}{2} \int_0^{2\pi} \int_\alpha^\beta \rho [U - \Theta] \sin 2\theta\, r dr d\theta + \frac{\rho_o}{2} \int_0^{2\pi} \int_\beta^{r_o} [U - \Theta] \sin 2\theta\, r dr d\theta$$

total y-momentum

$$\rho_i \int_0^{2\pi}\int_0^{\alpha} [U\sin^2\theta + \Theta\cos^2\theta]\, r dr d\theta + \int_0^{2\pi}\int_{\alpha}^{\beta} \rho[U\sin^2\theta + \Theta\cos^2\theta]\, r dr d\theta + \rho_o \int_0^{2\pi}\int_{\beta}^{r_o} [U\sin^2\theta + \Theta\cos^2\theta]\, r dr d\theta$$

using the fact that $\int_0^{2\pi}\sin\theta\cos\theta\, d\theta = 0$ and $\int_0^{2\pi}\sin^2\theta\, d\theta = \int_0^{2\pi}\cos^2\theta\, d\theta = \pi$ we have:

total mass

$$\rho_i\pi\alpha^2 + 2\pi\int_{\alpha}^{\beta}\rho(r)\, r dr + \rho_o\pi(r_o^2 - \beta^2)$$

total x-momentum

$$0$$

total y-momentum

$$\rho_i\pi\int_0^{\alpha}[U+\Theta]\, r dr + \pi\int_{\alpha}^{\beta}\rho(r)[U+\Theta]\, r dr + \rho_o\pi\int_{\beta}^{r_o}[U+\Theta]\, r dr$$

3. Conservation Equations: Applying the incompressibility constraint $d(rU(r))/dr = \Theta(r)$ the integral $\int_a^b [U(r)+\Theta(r)]\, r dr = \int_a^b [r^2U(r)]' dr = b^2U(b) - a^2U(a)$, the final conservation equations for the original (LHS) and modified droplet (RHS) are:

mass conservation

$$\rho_i r_i^2 + \rho_o(r_o^2 - r_i^2) = \rho_i\alpha^2 + 2\int_{\alpha}^{\beta}\rho(r)\, r dr + \rho_o(r_o^2 - \beta^2) \tag{29}$$

y-momentum conservation

$$-\rho_i r_i^2 U_0 = \rho_i\alpha^2 U(\alpha) + \int_{\alpha}^{\beta}\rho(r)[r^2U(r)]' dr + \rho_o[r_o^2U(r_o) - \beta^2U(\beta)] \tag{30}$$

2.4.2 Density Variation in $\alpha \le r \le \beta$

In the original droplet the density undergoes an abrupt change from ρ_i in the inner droplet to ρ_o in the outer ring. We propose to vary density gradually over the small radial distance $\beta - \alpha$ such that $\rho_{i-o} = \rho(r)$ only ($\partial\rho/\partial\theta = 0$) and is also independent of velocity.[6] The conditions the density must satisfy in this region are given by:

$$\rho(\alpha) = \rho_i, \quad \rho(\beta) = \rho_o \tag{31}$$

with the additional requirement of extra smoothness, i.e.:

$$\rho'(\alpha) = 0, \quad \rho'(\beta) = 0 \tag{32}$$

Proposing a polynomial density function with four unknown constant coefficients to satisfy the above four equations (31), (32) we have:

$$\rho(r) = a_0 + a_1 r + a_2 r^2 + a_3 r^3 \tag{33}$$

solving for the a_i's and noting that the density $\rho(r)$ depends on the parameters α, β, we obtain:

$$\rho_{\alpha\beta}(r) = \frac{\beta^2(\beta-3\alpha)\rho_i + \alpha^2(3\beta-\alpha)\rho_o}{(\beta-\alpha)^3} + \frac{6\alpha\beta(\rho_i-\rho_o)r}{(\beta-\alpha)^3} - \frac{3(\beta+\alpha)(\rho_i-\rho_o)r^2}{(\beta-\alpha)^3} + \frac{2(\rho_i-\rho_o)r^3}{(\beta-\alpha)^3} \tag{34}$$

where we must ensure $\beta \neq \alpha$ since $\rho(\alpha) = \rho_i$ whereas $\rho(\beta) = \rho_o$.

2.4.3 Solution for $U(r)$ and $\Theta(r)$ in $0 \le r \le r_o$

At the edge of the outer ring the velocities must vanish we have: $U(r_o) = 0$, $\Theta(r_o) = 0$ along with the incompressibility constraint:

$$U(r) = \frac{1}{r}\int_0^r \Theta(\xi)\, d\xi \tag{35}$$

with the integration constant being zero to ensure a finite central velocity. Note that the condition

[6] N.B. this problem remains an artificial one since the effect of viscosity, surface tension and convection are ignored. The current simplification could be expanded on through an extra coefficient in the density polynomial thereby including the effects of velocity implicitly although the velocity field, in this case, is purely a product of the incompressibility constraint.

$U(r_i) = -U_0$ has not been enforced and is only possible if the last term in (30) were to be identically zero. It is straightforward to include the zero boundary velocities into a polynomial approximation for Θ as well as a variation to take into account the two extra mass and momentum conservation equations (29) and (30). That is, let $\Theta(r) = (r_o - r)(b_0 + b_1 r)$. In addition to (35) the final three equations to solve for the unknown coefficients b_0, b_1 and the unknown radii α, β are respectively, upon simplification of (35) at $r = r_o$ as well as (29) and (30):

$$\int_0^{r_o} b_0(r - r_o) + b_1 r(r - r_o)\, dr = 0 \tag{36}$$

$$\int_\alpha^\beta \rho_{\alpha\beta}(r)\, r dr = \frac{\rho_i}{2}(r_i^2 - \alpha^2) + \frac{\rho_o}{2}(\beta^2 - r_i^2) \tag{37}$$

$$\int_\alpha^\beta \rho_{\alpha\beta}(r)[r^2 U(r)]' dr = \rho_o \beta^2 U(\beta) - \rho_i(r_i^2 U_0 + \alpha^2 U(\alpha)) \tag{38}$$

note that the mass conservation equation (37) is independent of velocity and as such is an equation for β in terms of α (or vice versa) so that both α and β cannot be chosen arbitrarily. Integrating we get:

$$[3\beta^2 + 4\alpha\beta - (10 r_i^2 - 3\alpha^2)](\rho_i - \rho_o) = 0$$

giving :

$$\beta = -\frac{2\alpha}{3} \pm \frac{\sqrt{30 r_i^2 - 5\alpha^2}}{3} \tag{39}$$

solving for the remaining coefficients b_0, b_1 we obtain for $U(r)$ and $\Theta(r)$:

$$U(r) = -\gamma_{\alpha\beta}(r - r_o)^2 \frac{\rho_i U_0}{\rho_i - \rho_o} \tag{40}$$

$$\Theta(r) = -\gamma_{\alpha\beta}(3r - r_o)(r - r_o)\frac{\rho_i U_0}{\rho_i - \rho_o} \tag{41}$$

where $\gamma_{\alpha\beta}$ is a constant with respect to r although a function of r_i and r_o and is dependent upon the parameters α and β:

$$\gamma_{\alpha\beta}(r_i, r_o) = \frac{70 r_i^2}{a r_o^2 + b r_o + c}$$

and

$$\begin{aligned} a &= 7(3\beta^2 + 4\alpha\beta + 3\alpha^2), \\ b &= -7(4\beta^3 + 6\alpha(\beta + \alpha)\beta + 4\alpha^3), \end{aligned} \tag{42}$$

$$c = 10(\beta^4 + \alpha^4) + 2\alpha\beta(8\beta^2 + 9\alpha\beta + 8\alpha^2) \tag{43}$$

then for any given $0 < \alpha \le r_i$ and $r_i \le \beta$ we choose the positive solution from (39), substitute into (40) and (41) to obtain computed values for $U(r), \Theta(r)$, where ρ_i, ρ_o, U_0 are all given beforehand. A pressure field may be found through the projection approach outlined in equations (7)-(10).

2.4.4 *Aspects of $U(r)$ and $\Theta(r)$*

1. Velocity at Droplet Center: Although the velocity at the center of the droplet for the OD case was $U(0) = \Theta(0) = -U_0$ we notice that at the center of the modified droplet the velocity is given by:

   $$U(0) = \Theta(0) = -\gamma_{\alpha\beta} r_o^2 \frac{\rho_i U_0}{\rho_i - \rho_o}$$

   so that the modified droplet velocity is determined by a ratio of ρ_i and ρ_o, as well as the radii α, r_o, r_i, and generally exceeds the original droplet velocity when the fraction $\gamma_{\alpha\beta} r_o^2 \rho_i / (\rho_i - \rho_o) > 1$.

2. Minimum and Maximum α and β: For the smallest possible value of $\alpha = 0, \beta = \sqrt{10/3} r_i$ so that:

   $$\gamma_{\alpha\beta} = \frac{63}{63 r_o^2 - 28\sqrt{30} r_i r_o + 100 r_i^2}$$

   with:

   $$U(r) = -\left(\frac{63(r - r_o)^2}{63 r_o^2 - 28\sqrt{30} r_i r_o + 100 r_i^2}\right)\frac{\rho_i U_0}{\rho_i - \rho_o},$$

   $$\Theta(r) = -\left(\frac{(3r - r_o)(r - r_o)}{63 r_o^2 - 28\sqrt{30} r_i r_o + 100 r_i^2}\right)\frac{\rho_i U_0}{\rho_i - \rho_o}$$

For the largest possible $\alpha = \beta = r_i$ we have:

$$\gamma_{\alpha\beta} = \frac{1}{(r_o - r_i)^2}$$

and the corresponding:

$$U(r) = -\left(\frac{r - r_o}{r_o - r_i}\right)^2 \frac{\rho_i U_0}{\rho_i - \rho_o},$$

$$\Theta(r) = -\left(\frac{(3r - r_o)(r - r_o)}{(r_o - r_i)^2}\right) \frac{\rho_i U_0}{\rho_i - \rho_o}$$

Note that the original droplet cannot be retrieved from the CSS solution when $\alpha = \beta = r_i$.

3. Restriction on r_o: Note that in the range $0 < r < r_o$ the minimum for both U and Θ is reached at $r = 0$ whereas the maximum for U is zero the maximum for Θ is obtained at $r = r_{tp}$ and $\Theta'(r_{tp}) = 0$, (where r_{tp} refers to the turning point) which occurs at $r_{tp} = 2r_o/3$ so that

$$\Theta(2r_o/3) = \left(\frac{\gamma_{\alpha\beta} r_o^2}{3}\right) \frac{\rho_i U_0}{\rho_i - \rho_o}$$

this peak is always less than or equal to U_0 when $(\rho_{io} = \rho_i - \rho_o)$:

$$r_o \geq \frac{3(\rho_{io})b - \sqrt{9\rho_{io}^2 b^2 + 12\rho_{io}[70\rho_i r_i^2 - 3\rho_{io} a]c}}{2[70\rho_i r_i^2 - 3\rho_{io} a]} \tag{44}$$

Using the previously defined values of a, b and c in (42) and (43). This ensures that $r_o - r_i \neq 0$ and also spreads the velocity over a larger range than the original droplet. It is this requirement that allows momentum conservation to be upheld.

2.4.5 *Solution for $u_x(x,y)$, $u_y(x,y)$*

Using the transformation equations (52) on the solutions (40) and (41) we get:

$$u_x(x,y) = \left(\frac{2\gamma_{\alpha\beta} xy(r - r_o)}{r}\right) \frac{\rho_i U_0}{\rho_i - \rho_o} \tag{45}$$

$$u_y(x,y) = -\left[\gamma_{\alpha\beta}\left(3x^4 + y^4 - 2(2x^2 + y^2) r_o r + 4x^2 y^2 + r_o^2 r^2\right) \Big/ r^2\right] \times \frac{\rho_i U_0}{\rho_i - \rho_o} \tag{46}$$

with

$$\Psi(x,y) = \gamma_{\alpha\beta} x (r - r_o)^2$$

3 Comparison of the Three Solutions

The three solutions, BCFS, SS and CSS, possess their own characteristics, these are summarized in Table 1 for a simple case of: inner droplet size α, transition region thickness $\beta - \alpha$, whether the method conserves mass and momentum, the percentage of the total momentum carried by the inner droplet and the minimum allowable size of the outer radius in order to ensure all velocities in Ω_o are less than or equal to U_0. The original droplet problem is used in Table 1 to act as a comparison.

Table 1: Properties of the example considered in Section 3.1.

Method Type	Method Characteristics			
	mass cons.	mom. cons.	% mom. in Ω_i	min. r_o
OD	yes	no	100	0.1
BCFS	yes	no	$\simeq 99.9$	$\simeq 0.29$
SS	yes	no	$\simeq 99.9$	$\simeq 0.31$
CSS	yes	yes	$\simeq 80$	$\simeq 0.24$

3.1 A Typical Case

The following example studies these properties by allocating specific values for the various parameters r_i, r_o, α and $U_0 = 1$ in a domain: $-1 \leq x, y \leq 1$ and a 100×100 grid ($h = \Delta x = \Delta y = 0.01$). The parameters for the OD, BCFS and SS cases are given by: $r_i = 0.1$, $r_o = 3.5 r_i$, $U_0 = 1$; whereas for the CSS: $\alpha = 0.8 r_i$ and the transition length $\beta - \alpha = 0.04 = 4h$, four integer multiples of the cell width. Note that for the OD, BCFS and SS cases α and β have been chosen as constant, $\alpha = \beta = r_i$, and it is in the CSS case, where the

velocity is radially dependent, that a gradual density variation is considered most relevant.

From Table 1 several clear conclusions can be drawn: firstly, only the CSS conserves both mass and momentum, whereas mass must be conserved as a matter of course, momentum is an associated physical property which we would like to have conserved as part of the problem solution. Secondly, in all cases, except the CSS, virtually all of the momentum is carried by the inner droplet. Thirdly, the minimal allowable outer radius for the CSS is the smallest of all whereas both the BCFS and SS have larger requirements.

3.1.1 $U(r)$, $\Theta(r)$ Characteristics

Figure 3, shows, in addition, that the velocity at the center of the droplet for the CSS case, $|\mathbf{u}_{CSS}(0,\theta)| \simeq 2$, exceeds the original droplet velocity, $|\mathbf{u}_{OD}(0,\theta)| = U_0 = 1$, although remaining within the same order of magnitude as the original. Whereas all of the $U(r)$ curves show much the same general form, except for the fact that $U_{CSS}(\alpha) < U_{BCFS}(\alpha), U_{SS}(\alpha) = -U_0$, those for $\Theta(r)$ vary significantly with the CSS case being lower in maximum magnitude than either of the other two cases and SS being larger than either of the other two. Similarly, the velocity for the CSS case is spread out over the whole range, $0 \leq r \leq r_o$, allowing the lowering of the maximum size but also increasing the vertical velocity at the center of the droplet and creating a change in velocity from the center outwards. Note that computational experiments also show that more of the momentum for the BCFS case is confined near the original droplet than in either of the other two cases which progressively spread the velocities further out.

3.1.2 Stream Functions

U and Θ as function of radius measured from the center of the droplet for all three solution types for the given parameters $r_i = 0.1$, $r_o = 3.5r_i$, $U_0 = 1$, $\alpha = 0.8r_i$ with its associated $\beta = 1.2r_i$.

Further characteristics of the solutions are shown in Figures 4 and 5 where the stream function for each of the solution types is compared with the original droplet. Clearly, the qualitative characteristics of the stream function for each of the solutions is similar showing vertical streamlines within the inner droplet for the BCFS and SS cases, although diverging from the vertical for the CSS case, surrounded by recirculating streamlines in the outer ring which match at $r = r_i$. This recirculation pattern in the outer ring is a product of the creation of a flow field which ensures the div-free condition is satisfied within the whole domain. This is also justified in a physical sense since boundary layer theory requires that outside of the inner droplet the velocity should not be immediately zero.

3.1.3 Method Divergence

Table 2 shows the maximum discrete divergence calculated using the second order central difference operator $D_{i,j} \cdot \mathbf{u} = (u_{i+1,j} - u_{i-1,j})/2h + (v_{i,j+1} - v_{i,j-1})/2h$ which, given a finite grid spacing, calculates both a large finite divergence for the OD case, rather than an infinite result, and a non-zero divergence for the analytically exact div-free BCF, S and CS Solutions. In this sense all solution types vastly improve the calculated maximum discrete divergence, $||D_{i,j} \cdot \mathbf{u}||_\infty$, when compared to the very large result of the OD.

Table 2: The maximum divergences of each method.

Method Type	$\|\|D_{i,j} \cdot \mathbf{u}\|\|_\infty$
OD	50
BCFS	5.5×10^{-16}
SS	6.6×10^{-16}
CSS ($\alpha = 0.8$)	6.9×10^{-16}

This can also be seen graphically in Figures 6 and 7 which shows contour plots of the numerically calculated divergence field, $D_{i,j} \cdot \mathbf{u}$ in each case. The reason that no contour lines, other than a cloud of the darker region for $r_i < r < r_o$, are clearly visible in Figures 6(b), 7(a) and $0 < r < r_o$ for 7(b), is that the values of the calculated divergence are extremely small. But, they are nevertheless non-zero throughout and larger within the outer ring, whereas the values of the calculated

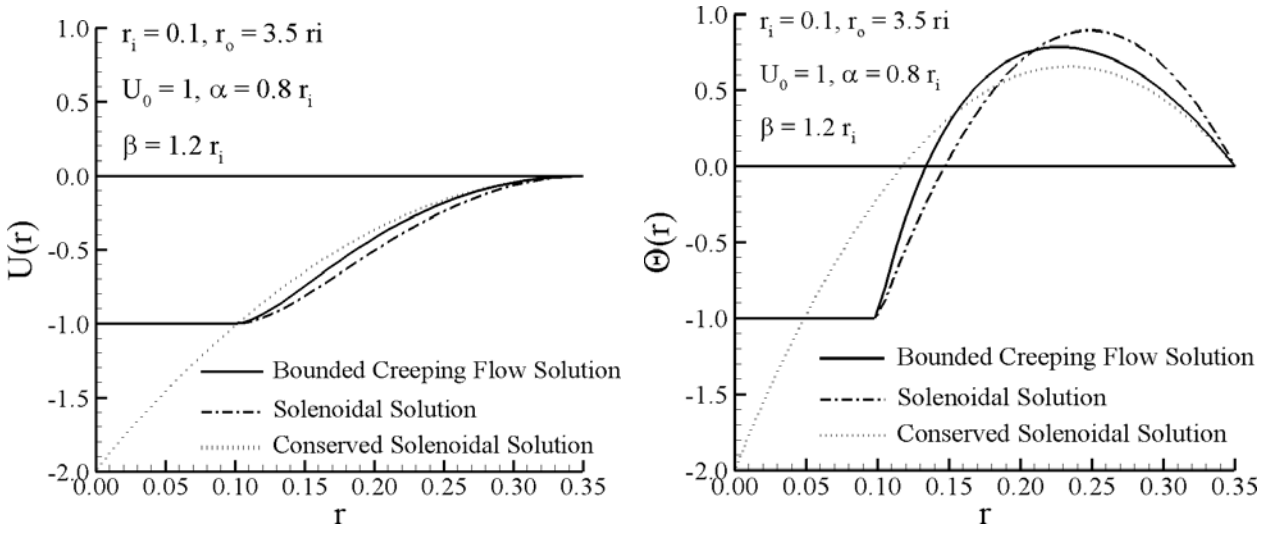

(a) $U(r)$ (b) $\Theta(r)$

Figure 3: U and Θ as function of radius measured from the center of the droplet for all three solution types for the given parameters $r_i = 0.1$, $r_o = 3.5r_i$, $U_0 = 1$, $\alpha = 0.8r_i$ with its associated $\beta = 1.2r_i$.

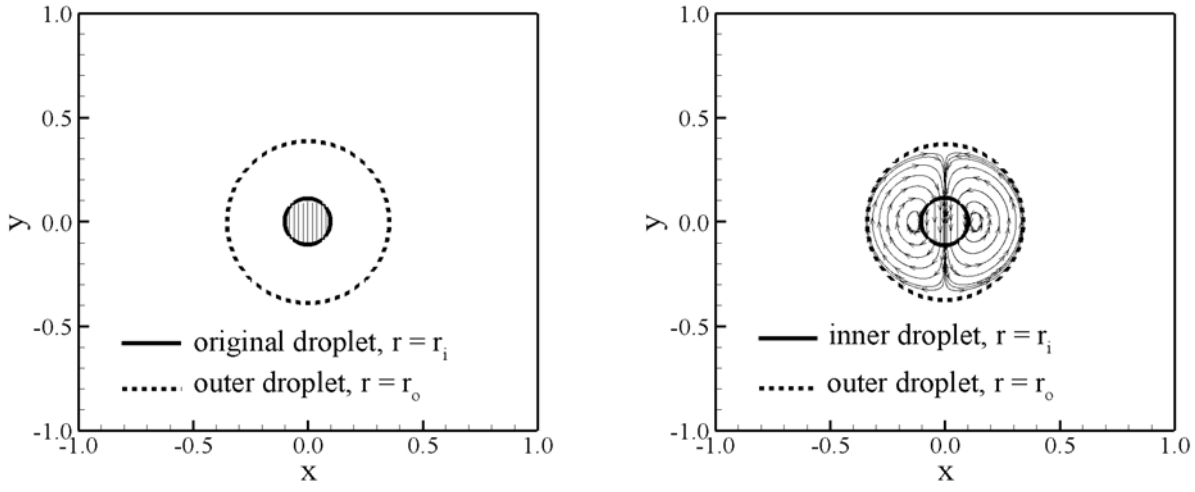

(a) original droplet (b) BCF solution

Figure 4: Stream function $\Psi(x,y)$ indicating the flow within the inner and outer droplet for each problem type: (a) the Original Droplet, (b) the Bounded Creeping Flow Solution

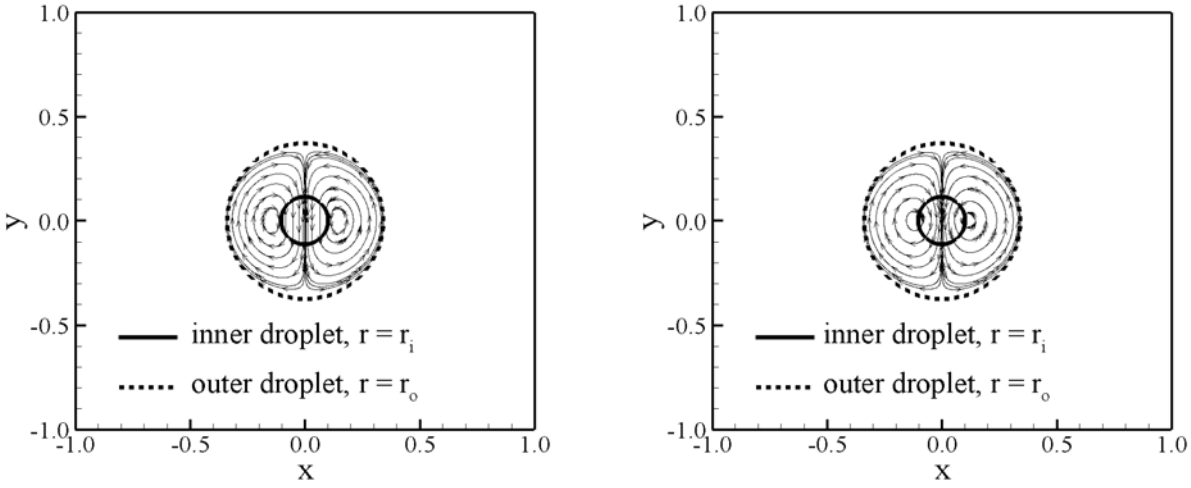

(a) solenoidal solution (b) CS solution

Figure 5: Stream function $\Psi(x,y)$ indicating the flow within the inner and outer droplet for each problem type: (c) The Solenoidal Solution and (d) The Conserved Solenoidal Solution.

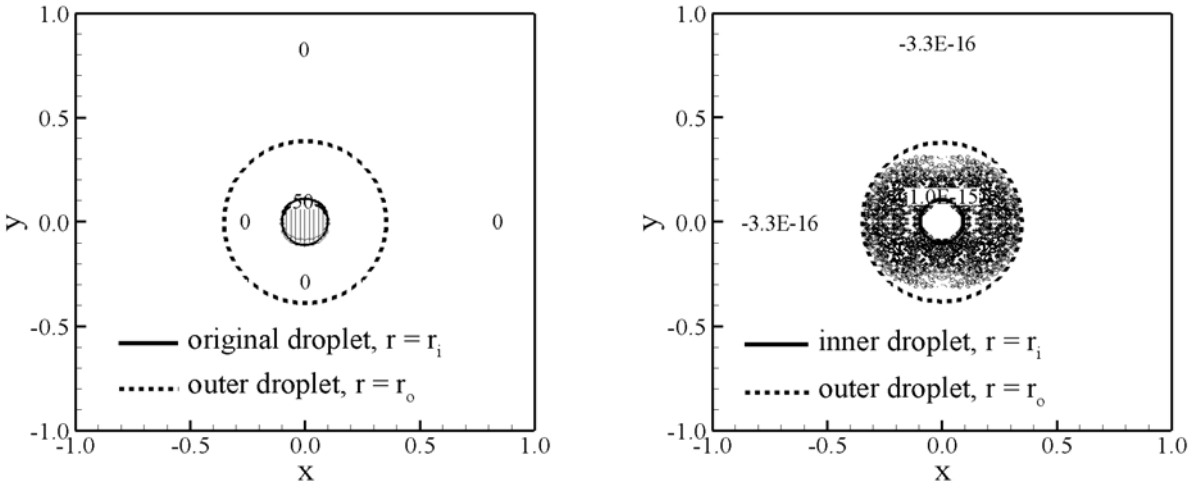

(a) original droplet (b) BCF solution

Figure 6: Contour plots of the numerically calculated divergence $D_{i,j} \cdot \mathbf{u}$ for each solution type: (a) the Original Droplet, (b) the Bounded Creeping Flow Solution

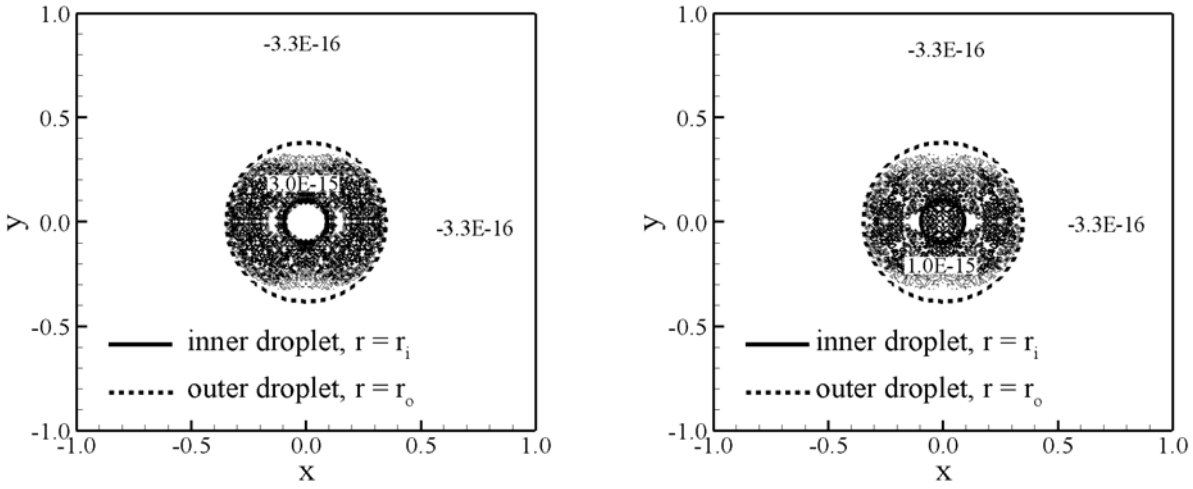

(a) solenoidal solution (b) CS solution

Figure 7: Contour plots of the numerically calculated divergence $D_{i,j} \cdot \mathbf{u}$ for each solution type: (c) The Solenoidal Solution and (d) The Conserved Solenoidal Solution

divergence in Figure 6(a) is clearly zero. Furthermore, we have noticed that both the BCFS and SS cases have divergences of the same average size confined within the ring $r_i < r < r_o$ whereas the CSS case has a larger divergence by a factor of about 2 and spreads non-zero divergences over $0 < r < r_o$ with much of the larger values within the inner droplet.

3.1.4 Advantages and Disadvantages

Tables 3 and 4 lists some of the clear advantages and disadvantages of the various solution types.

It would appear that the least successful case is CSS, the best is BCFS with SS in between. However, it must be emphasized that some of these aspects are more important than others. The fact that momentum is conserved in the CSS case and that it possesses the smallest minimum r_o count strongly in its favor. The actual usefulness of each has been tested conclusively by running dynamical tests of the full NS free-surface problem and the detailed results are to be presented in a forthcoming paper.

Table 3: Advantages of the three solutions considered.

Method	Advantages
BCFS	1. small divergence in outer ring 2. zero divergence in inner droplet 3. inner vertical velocity $-U_0$ 4. most momentum in inner droplet 5. remaining momentum near r_i
SS	1. small divergence in outer ring 2. zero divergence in inner droplet 3. inner vertical velocity $-U_0$ 4. most momentum in inner droplet
CSS	1. lowest minimum r_o 2. conserves momentum

4 Discussion and Conclusions

All of the analytical solutions studied in this paper, the BCFS, SS and the CSS, provide acceptable approximations to the initial state of the original droplet with uniform vertical velocity. In addition, they all conserve mass by strictly obeying the incompressibility constraint and satisfy the re-

Table 4: Disadvantages of the three solutions considered.

Method	Disadvantages
BCFS	1. larger minimum r_o 2. doesn't conserve momentum
SS	1. largest minimum r_o 2. doesn't conserve momentum 3. remaining momentum spread out
CSS	1. larger divergence in inner & outer ring 2. non-zero divergence in inner droplet 3. inner non-vertical velocity $< -U_0$ 4. some momentum in outer ring 5. remaining momentum spread out

quirement of no slip at the domain boundary by attaining zero velocity within a small number of droplet radii beyond the original droplet edge. In each case it was found that the ring-droplet width, $r_o - r_i$, could not be reduced below a certain size based on the criterion of Section 2.2.3 that the largest possible velocity could not exceed the vertical velocity of the initial state U_0. This is a product of the restriction on the size of the velocity field at the domain boundary as well as an attempt to maintain, as much as possible, the characteristics of the original droplet. Such a requirement is not satisfied by the original creeping flow solution for the translating solid sphere which allows an asymptotic decay of the radial velocity component. These constraints on the solution gave rise to an outer ring of fluid which allowed a smooth transition from a finite inner droplet of uniform vertical velocity to zero velocity beyond the ring in order to satisfy the div-free constraint. Although this constraint appears, at first, to allow the creation of unphysical solutions this was not found to be the case. All of the solution types maintain a velocity field of the order of the original droplet, carry almost all of the momentum and mass within a radius equivalent to the original droplet and in the case of CSS also conserve momentum exactly. A consequence of this method of solution is the fact that for all of the solution types the stream functions obtained resemble the inner circulation present in a translating fluid sphere of radius r_o (rather than r_i) with the mass and momentum mostly confined within the smaller radius r_i.

While the BCF Solution actually obeys the NS equations it is the most difficult to obtain of all of the solution types. On the other hand the Solenoidal Solution is both simple to obtain and provides at least a practical initial condition for the solution of two-phase interfacial flow problems. Finally, the Conserved Solenoidal Solution attempts to alleviate the weaknesses of both the BCFS and SS cases by being easier to solve than the BCFS case and also retaining more of the physical properties than the SS case. Based on the preliminary results of this paper the Solenoidal Solution provides the simplest and most cost effective solution to the problem of an initial condition for the numerical solution of the NS equations in two-phase flow. A better recommendation would be possible upon numerical testing of all solution types in an interfacial flow problem.

The approach used in this paper to obtain a realistic initial condition for interfacial flow problems may be extended further by considering two-phase flows with more general geometries as well as a study of three dimensional flows. As well, the projection of non-solenoidal, discontinuous velocity fields situated within a discontinuous density field warrants further research, even in one dimension. There also remains the possibility of including the conservation of energy within the CS Solution through extra constraint equations in Section 2.4.1 and the addition of an extra coefficient in the polynomial approximation of $\Theta(r)$.

References

Aleinov, I.; Puckett, E. G. (1995): Computing surface tension with higher-order kernels. In *Proc. 6th International Symposium on Computational Fluid Dynamics*, Lake Tahoe, CA.

Almgren, A. S.; Bell, J. B.; Szymczak, W. G. (1996): A Numerical Method for the Incompressible Navier-Stokes Equations Based on an Approximate Projection. *SIAM J. Sci. Comput.*, vol. 17, pp. 358–369.

Anderson, D. M.; McFadden, G. B.; Wheeler, A. A. (1998): Diffuse-Interface Methods in Fluid Mechanics. *Annu. Rev. Fluid Mech.*, vol. 30, pp. 139–165.

Bell, J. .; Colella, P.; Glaz, H. M. (1989): A Second-Order Projection Method of the Incompressible Navier-Stokes Equations. *J. Comput. Phys.*, vol. 85, pp. 257–283.

Bell, J. B.; Marcus, D. L. (1992): A Second-Order Projection Method for Variable-Density Flows. *J. Comput. Phys.*, vol. 101, pp. 334–348.

Bierbrauer, F. (2004): *Mathematical Modelling of Water-Droplet Impact on Hot Galvanised Steel Surfaces*. University of Wollongong, Wollongong, Australia.

Bierbrauer, F.; Soh, W. K.; Yuen, W. Y. D. (2002): An Eulerian-Lagrangian Method for Convective Heat Transfer at a Stagnation Point. *Comput. Fluid Dyn. J.*, vol. 10, pp. 446–453.

Chorin, A. J. (1968): Numerical Solution of the Navier-Stokes Equations. *Math. Comput.*, vol. 22, pp. 745–762.

Frohn, A.; Roth, A. N. (2000): *Dynamics of Droplets*. Springer, New York.

Gresho, P. M. (1990): On the Theory of Semi-Implicit Projection Methods for Viscous Incompressible Flow and its Implementation Via a Finite Element Method that Also Introduces a Nearly Consistent Mass Matrix, Part 1: Theory. *Int. J. Numer. Methods Fluids*, vol. 11, pp. 587–619.

Gresho, P. M. (1991): Some Current CFD Issues Relevant to the Incompressible Navier-Stokes Equations. *Comput. Methods Appl. Mech. Eng.*, vol. 87, pp. 201–252.

Gresho, P. M. (1992): Incompressible Fluid Dynamics: Some Fundamental Formulation Issues. *Annu. Rev. Fluid Mech.*, vol. 23, pp. 413–453.

Gresho, P. M.; Sani, R. (1987): On Pressure Boundary Conditions for the Incompressible Navier-Stokes Equations. *Int. J. Numer. Methods Fluids*, vol. 7, pp. 1111–1145.

Happel, J.; Brenner, H. (1991): *Low Reynolds Number Hydrodynamics*. Kluwer, London.

Hyman, J.; Shashkov, M.; Steinberg, S. (1997): The Numerical Solution of Diffusion Problems in Strongly Heterogeneous Non-Isotropic Materials. *J. Comput. Phys.*, vol. 132, pp. 130–148.

Kothe, D. B. (1999): Perspectives on eulerian finite volume methods for incompressible interfacial flows. In Kuhlmann, H. C.; Rath, H. J.(Eds): *Free Surface Flows*, New York. Springer.

Kothe, D. B.; Rider, W. J. (1995): Practical considerations for interface tracking methods. In *Proc. 6th International Symposium on Computational Fluid Dynamics*, Lake Tahoe, CA.

Leal, L. G. (1992): *Laminar Flow and Convective Transport Processes*. Butterworth-Heinemann, Boston.

Li, Z. (1994): *The Immersed Interface Method - A Numerical Approach for Partial Differential Equations with Interfaces*. University of Washington, Washington.

Prosperetti, A. (2000): Navier-stokes numerical algorithms for free-surface flow computations: An overview. In Rein, M.(Ed): *Drop-Surface Interactions*, New York. Springer.

Puckett, E. G.; Almgren, A. S.; Bell, J. B.; Marcus, D.; Rider, W. J. (1997): A High-Order Projection Method for Tracking Fluid Interfaces in Variable Density Incompressible Flows. *J. Comput. Phys.*, vol. 130, pp. 269–282.

Quartapelle, L. (1993): *Numerical Solution of the Incompressible Navier-Stokes Equations*. Birkhäuser, Basel.

Reddy, B. D. (1998): *Introductory Functional Analysis: with Applications to Boundary Value Problems and Finite Elements*. Springer, New York.

Rider, W. J. (1994): Approximate Projection Methods for Incompressible Flow: Implementation, Variants and Robustness. Technical Report LA-UR-2000, Los Alamos, LANL, NM, 1994.

Rider, W. J.; Kothe, D. B.; Mosso, S. J.; Cerutti, J. H.; Hochstein, J. I. (1995): Accurate solution algorithms for incompressible multifluid flows. In *33rd Aerospace Sciences Meeting*, Reno, NV.

Scardovelli, R.; Zaleski, S. (1999): Direct Numerical Simulation of Free-Surface and Interfacial Flow. *Annu. Rev. Fluid Mech.*, vol. 31, pp. 567–603.

Sohr, H. (2000): *The Navier-Stokes Equations: An Elementary Functional Analytical Approach*. Birkhäuser, Basel.

Temam, R. (1985): *Navier-Stokes Equations*. North-Holland, Amsterdam.

Vincent, S.; Caltagirone, J. P. (2000): A One-Cell Local Multigrid Method for Solving Unsteady Incompressible Multiphase Flow. *J. Comput. Phys.*, vol. 163, pp. 172–215.

Wang, W. C. (2004): A Jump Condition Capturing Finite Difference Scheme for Elliptic Interface Problems. *SIAM J. Sci. Comput.*, vol. 25, pp. 1479–1496.

Zhu, S. P. (2001): An Innovative Open Boundary Treatment for Nonlinear Water Waves in A Numerical Wave Tank. *CMES: Computer Modeling in Engineering and Sciences*, vol. 2, pp. 227–236.

Appendix A: The Non-Solenoidality of the Initial State

The fact that the initial state is not divergence free can be demonstrated with the use of distribution theory Reddy (1998). Consider the unit domain $\Omega = \{(x,y) : 0 \le x,y \le 1\}$, containing two distinct subdomains such that $\Omega = \Omega_a \cup \Omega_d$, where Ω_a corresponds to the ambient (a) fluid surrounding the droplet (d) which is located in Ω_d as shown in Figure 1.

The initial state may be defined, for $\mathbf{u}_0 \in L^2(\Omega)$, as $\mathbf{u}_0(\mathbf{x}) = -\chi_{\Omega_d}(\mathbf{x})U_0\mathbf{j}$, where

$$\chi_{\Omega_d}(\mathbf{x}) = \begin{cases} 1 & \text{if} \quad \mathbf{x} \in \Omega_d \\ 0 & \text{if} \quad \mathbf{x} \notin \Omega_d \end{cases} \tag{47}$$

is the characteristic function. To show that the initial state is not solenoidal, consider the divergence in the sense of distributions. Now the velocity is purely vertical so that $\nabla \cdot \mathbf{u}_0 = -U_0 \partial\left(\chi_{\Omega_d}(\mathbf{x})\right)/\partial y$. Then consider a set of test functions $\phi(\mathbf{x})$ that are $C_0^\infty(\Omega)$ i.e. the set of infinitely differentiable functions with compact support. Then:

$$\langle \nabla \cdot \mathbf{u}_0, \phi \rangle = -U_0 \int_\Omega \frac{\partial \chi(\mathbf{x})}{\partial y} \phi \, d\mathbf{x} = U_0 \int_{\Omega_d} \frac{\partial \phi}{\partial y} \, d\mathbf{x}$$

using a coordinate system centered at the origin of the spherical droplet of given radius R, we obtain:

$$\begin{aligned} \langle \nabla \cdot \mathbf{u}_0, \phi \rangle &= U_0 \int_{-R}^{R} \int_{-\sqrt{R^2-x^2}}^{\sqrt{R^2-x^2}} \frac{\partial \phi}{\partial y} \, dy\, dx \\ &= U_0 \int_{-R}^{R} \phi(x, \sqrt{R^2-x^2}) - \phi(x, -\sqrt{R^2-x^2}) \, dx \\ &\neq 0 \end{aligned} \tag{48}$$

so $\nabla \cdot \mathbf{u}_0 \neq 0$ since there exists ϕ such that (48) is not equal to zero, Reddy (1998).

Appendix B: Polar Coordinates in the Initialization Problem

Let the origin of the coordinate system lie at the center of the droplet, of radius r_i, in a stationary frame such that:

$$x = r\cos\theta, \quad y = r\sin\theta$$

for $0 \le \theta \le 2\pi$, $0 \le r \le r_o$, where r_o is the maximum radius, then the velocity vector may be written as:

$$\mathbf{u}(r,\theta) = u_r(r,\theta)\mathbf{r} + u_\theta(r,\theta)\theta$$

for unit vectors $\mathbf{r}$ and θ in the radial and azimuthal directions. Note the transformation from and to $x-y$ coordinates as:

$$\begin{aligned} u_x &= u_r\cos\theta - u_\theta\sin\theta, \\ u_y &= u_r\sin\theta + u_\theta\cos\theta \\ u_r &= u_x\cos\theta + u_y\sin\theta, \\ u_\theta &= -u_x\sin\theta + u_y\cos\theta \end{aligned} \tag{49}$$

for components $u_r = u_r(r,\theta)$, $u_\theta = u_\theta(r,\theta)$, $u_x = u_x(x,y)$ and $u_y = u_y(x,y)$. Similarly, the divergence-free constraint reads:

$$\nabla \cdot \mathbf{u} = \frac{\partial (r u_r)}{\partial r} + \frac{\partial u_\theta}{\partial \theta} = 0 \tag{50}$$

Since the original droplet possesses a constant vertical velocity expressible in polar coordinates as:

$$\mathbf{u} = -U_0 \mathbf{j} = -U_0 \sin\theta \mathbf{r} - U_0 \cos\theta \theta$$

this suggests the simplification:

$$u_r = U(r)\sin\theta, \quad u_\theta = \Theta(r)\cos\theta \tag{51}$$

so that:

$$\begin{aligned} u_x &= [U(r) - \Theta(r)]\sin\theta\cos\theta, \\ u_y &= U(r)\sin^2\theta + \Theta(r)\cos^2\theta \end{aligned} \tag{52}$$

and the div-free equation becomes

$$\frac{d(rU(r))}{dr} = \Theta(r) \tag{53}$$